



ORIGINAL ARTICLE

Postoperative Positional and Dimensional Changes of Mandibular Canal after Bilateral Sagittal Split Set-Back Osteotomy

Duygu İşcan¹, Melih Motro², Ahu Acar³

¹Private Practice, Istanbul, Turkey

²Department of Orthodontics and Dentofacial Orthopedics, Boston University School of Dental Medicine, MA, USA

³Department of Orthodontics, Marmara University School of Dentistry, Istanbul, Turkey

Cite this article as: İşcan D, Motro M, Acar A. Postoperative Positional and Dimensional Changes of Mandibular Canal after Bilateral Sagittal Split Set-Back Osteotomy. Turkish J Orthod 2017; 30: 110-7.

ABSTRACT

Objective: This preliminary study was planned to provide information about preoperative mandibular canal (MC) position and the postoperative positional changes of MC and length in three dimensions, with the purpose of providing some assistance in reducing inferior alveolar neurosensory disturbance (IAND).

Methods: MC was examined on CBCT data using SimPlant Pro Standalone 13.0. MC locations were measured in all dimensions, with respect to mandibular bony borders.

Results: The results showed that MC is frequently located in the midthird of the ramus anteroposteriorly and superoinferiorly and in the midthird of the corpus superoinferiorly. Postoperatively, ramus width was increased, ramus length was decreased significantly, and MC was repositioned laterally and inferiorly. MC length was decreased on both sides, non-correlated with the set-back amounts.

Conclusion: Preoperative results may be beneficial for the prediction of MC position for surgeons, and postoperative results will be used for the following studies to correlate postoperative positional changes with IAND.

Keywords: Orthognathic surgery, mandibular canal, bilateral sagittal split osteotomy, set-back surgery, cone-beam computed tomography, 3D imaging

INTRODUCTION

Orthognathic surgery is the only treatment protocol for severe Skeletal Class III. Orthognathic surgical plan is determined according to the origin of the malocclusion; maxillary advancement for maxillary retrognathism, mandibular setback for mandibular prognathism, or double jaw surgery for both maxillomandibular deformities.

The most common technique that has been used since 1957 is the bilateral sagittal split ramus osteotomy (BSSO) (1-5).

Besides the advantages of bilateral sagittal split osteotomy technique, BSSO is also a detailed and sensitive technique where there is also a high risk for postoperative IAND as a result of manipulation of the nerve during operation (2-5).

As a spontaneous result of BSSO, IAND occurs in the short term with 100% incidence as the most common complication of BSSO. Mandibular canal (MC) is in close proximity with the osteotomy region of the BSSO technique, leading to a high risk of inferior alveolar nerve (IAN) injury (6-12).

Anatomical knowledge on the location of the vascular and nerve bundles in the frontal plane for reducing or eliminating the risk of an injury to the nerve during BSSO can be obtained by visualizing the MC by panoramic radiography or 3D techniques. Tamas (13) used dry skulls to show the location and adjacency of MC. Liu et al. (12)

showed the distribution of linear, spoon shape, elliptic arc, and turning curve types of MC related with the risk of injury.

Panoramic radiography was used to visualize the different pathways of MC (10); however, this technique is a limited way of MC imaging because of the distortions caused by magnification (12, 14). Because of this limitation, many authors used 3D imaging techniques despite high doses and prices. (6, 8, 11, 15-18). Yamamoto et al. (15) determined the location of MC on predefined slices and showed an increased risk of IAND when MC is in contact with external cortical bone of the mandible. Witter et al. (16) also used the CT images to examine the MC and determined that if the distance between the MC and the inner surface of the cortical bone was less than 1 mm or if the canal contacted the external cortical bone, it was registered as a possible neurosensory compromising proximity. Muto et al. (8) examined ramus morphology on BT images and showed the safest region to establish the medial osteotomy line as just superior and 5 to 6 mm posterior to the lingula, directing the line slightly inferior. Tsuji et al. (11) also used BT images to figure out the safest region for buccal corticotomy and showed it as the anterior proximity of mandibular angle. Ueki et al. (17) revealed the postoperative changes on MC location on BT images. Yoshioka et al. (18) examined the relationship between IAND and the bone quality and position of MC using the 2-mm thickness of continuous sections on CT images and found that if the Hounsfield unit (HU) values around the MC were greater than 300 HU and/or the distance from the buccal aspect of the MC to the outer buccal cortical margin was less than 6 mm, IAND at 1 year after BSSO would be significantly increased.

Computerized tomography is the best technique of MC imaging with high-quality views. But high radiation doses and prices of MS computed tomography led clinicians to prefer CBCT in their assessments, despite its lower quality view due to lower radiation doses (19). A study examining the visibility of MC on CBCT images revealed that MC was clearly visible in 53% of the hemi-mandibles and difficult and very difficult visualizations were registered in 25% and 22% of the hemi-mandibles, respectively. The visibility of the MC on distal regions was superior when compared to regions closer to the mental foramen (20).

Aizenbud et al. (21) investigated the difference of IAND between the surgeries in which the precise MC position was determined on CBCT images preoperatively and those in which no preoperative assessment was made. They found a significant reduction in IAND in the surgeries in which the MC positions were precisely determined preoperatively.

The aim of this study was to define the preoperative MC trajectory and to evaluate postoperative changes of MC length and location after setback surgery.

METHODS

The study material consisted of CBCT images of 21 individuals, obtained from the archives of Marmara University Faculty of Dentistry Department of Orthodontics. Of these 21 individuals, 7 were men (33.3%) and 14 (66.7%) were women, with a mean age of 24.05 ± 5.85 y (min-max, 18-37 y). Inclusion criteria were: (i) no medical problems, (ii) no congenital syndromes, (iii) having undergone mandibular setback surgery with BSSO, and (iv) having pre- and post-op high-quality CBCTs. The CBCTs have

been obtained preoperatively and 3 to 6 months after surgery as part of the routine protocol for orthognathic surgery patients. The present study has been approved by the Ethical Committee of the Health Sciences Institute of Marmara University, and the informed consent forms have been taken.

Surgical Procedure

Orthognathic surgeries had been performed by two plastic and reconstructive surgeons. According to the information obtained from the surgeons, a modified BSSO technique was used with the purpose of preventing IAN injuries, precisising splitting, enlarging the bony segment surfaces, thus enhancing rigid fixation, and postoperative healing. The surgical technique used was a modified BSSO technique of Trauner and Obwegeser's (1) classical BSSO technique by Dal Pont's anteriorly positioned vertical cut and Epker's complete osteotomy of the inferior mandibular cortex.

Three-Dimensional Examination

CBCT images were taken 1 week before surgery and 10 and 22 weeks after surgery. The technical properties of the CBCT machine used (Iluma Imtec, 3M, St Paul, Minn) were as follows: focal spot: 0.3 mm \times 0.3 mm; X-ray tube working with 120 KV; X-ray tube current: 1-4 mA; detector size: 19.5 cm \times 24.5 cm; scanning with 360° rotation; radiation: 555 microsieverts maximum; scanning time, 40 s maximum and 7.8 s minimum; field of view or imaging area: 14.2 cm \times 21.1 cm; voxel size: 0.0936 mm; and gray scale: 14 bit. The CBCT data obtained had been saved as DICOMs and viewed on SimPlant®Pro 13.0 (Materialise Dental NV, Leuven, Belgium).

Three-dimensional (3D) evaluations and measurements were performed by the same operator, DI. First step was to standardize the head position on pre- and post-op CBCT images. By "Reorientation" option, mandibular occlusal plane was orientated parallel to the horizontal plane on coronal and sagittal images, and the midsagittal plane was oriented parallel to the vertical plane on axial images. The following step was drawing panoramic curve, and obtaining ideal panoramic view, by "Draw/Manipulate Panoramic Curve" option. Panoramic curve was determined by indicating the center of the MC, from mandibular foramen to mental foramen on both sides, to derive maximum buccolingual size of MC on ideal panoramic view. The next step was to get mandibular nerve as a 3D object. The MC was plotted on the ideal panoramic view by "Draw/Manipulate Nerve" option. The plottings were corrected on every transaxial slice and the 3D MC object was derived.

Measurements

All the measurements were performed by the same operator, DI. Pre- and post-op MC locations were determined by measuring the distances between MC and mandibular bony borders. These measurements were performed at one axial and four cross-sectional slices. Axial slice (AS) and first cross-sectional slice (CS1) were taken at the most inferior point of mandibular foramen; other cross-sectional slices were taken at the midpoint between the mandibular foramen and the distal point of the mandibular second molar (CSM), at the distal point of mandibular second molar (CS7), and at the contact point of mandibular first and second molars (CS7-6) (Figure 1).

The measurements at all slices were the distance between the most inferior and superior point of ramus/corpus (RL/CoL: Ramus/Corpus Length), the distance between the most distal and medi-

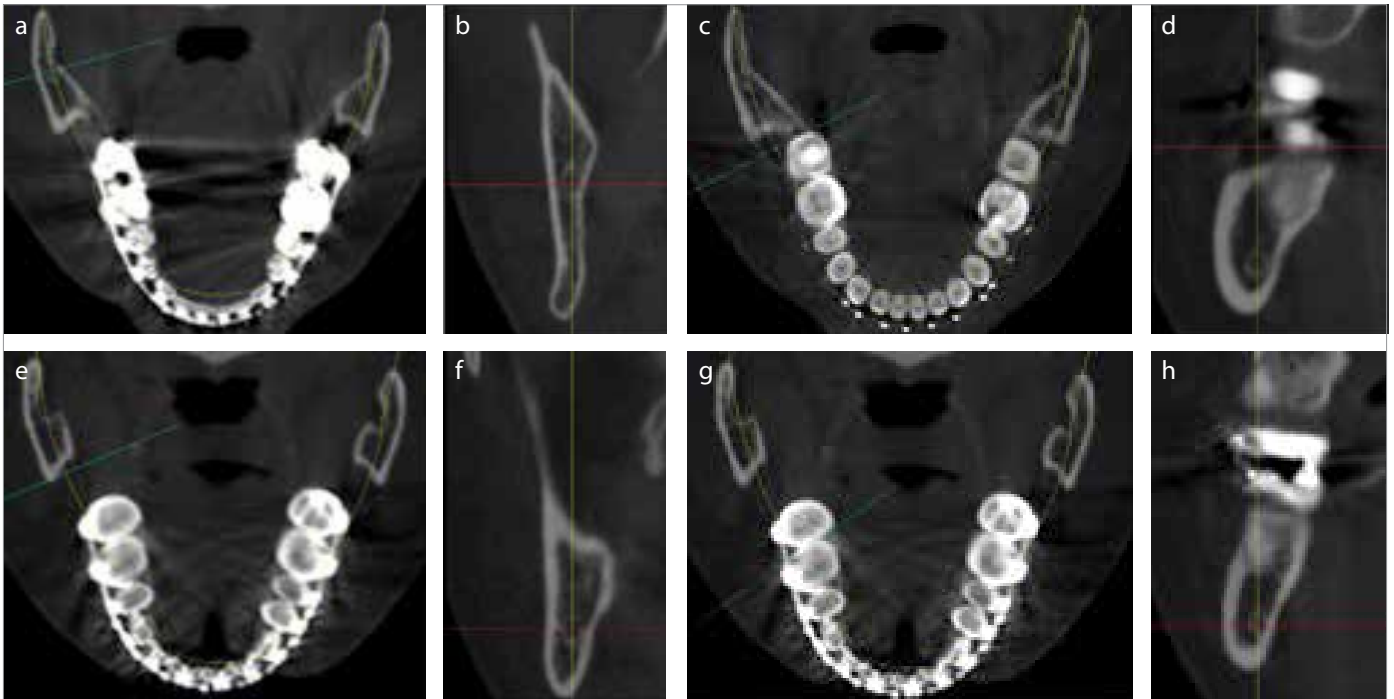


Figure 1. a-h. Axial slice (AS) taken from the most inferior point of mandibular foramen (a); first cross-sectional slice (CS1) taken from the same point as AS (b); the most distal point of mandibular second molar (c); cross-sectional slice distal to the mandibular second molar (CS7) (d); the midpoint between CS1 and CS7 (e); cross-sectional midslice (CSM) between CS1 and CS7 (f); the contact point of mandibular second molar and mandibular first molar (g); and cross-sectional slice in between mandibular second and first molars (C7-6) (h)

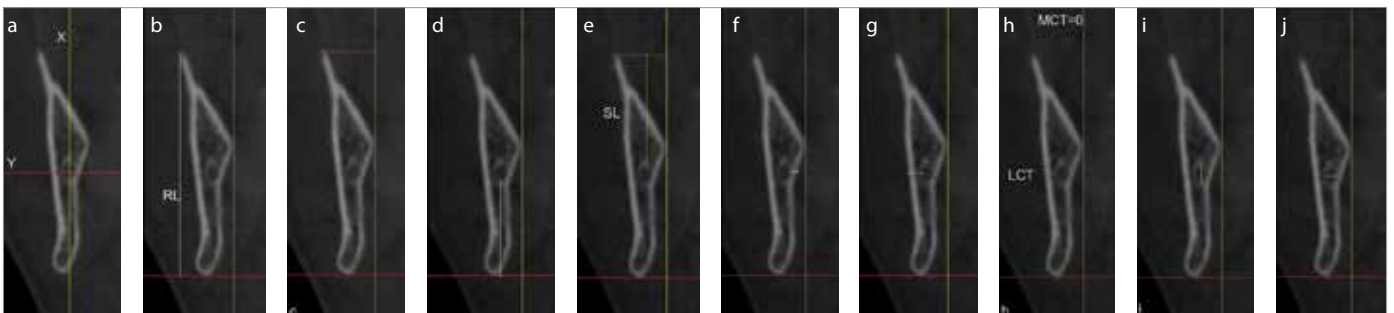


Figure 2. a-j. Reference planes for cross-sectional slices (a); ramus length (b); ramus width (c); inferior length (d); superior length (e); medial length (f); and lateral length (g); medial and lateral cancellous bone thickness (h); canal length (i); and canal width (j)

al points of ramus/corpus (RW/CoW: Ramus/Corpus Width), the distance between the most posterior outer cortical point of MC and the posterior bony border of the mandible in axial slices (PL: Posterior Length), the distance between the most inferior outer cortical point of MC and the inferior bony border of the mandible (IL: Inferior Length), the distance between the most anterior outer cortical point of MC and the anterior bony border of the mandible in ASs (AL: Anterior Length), the distance between the most superior outer cortical point of MC and the superior bony border of the mandible (SL: Superior Length), the distance between the most medial outer cortical point of MC and the medial bony border of the mandible (ML: Medial Length), the distance between the most distal outer cortical point of MC and the lateral bony border of the mandible (LL: Lateral Length), the distance between the most medial outer cortical point of MC and the medial inner bony border of the mandible (MCT: Medial Cancellous Bone Thickness), the distance between the most distal outer cortical point of MC and the distal inner bony border of the mandible (LCT: Lateral Cancellous Bone Thickness), the distance between

the most inferior and superior inner cortical bone points (CL: Canal length), and the distance between the most medial and distal inner cortical bone points (CW: Canal Width) (Figure 2).

Proportional evaluation of MC locations was performed on ASs and cross-sectional slices taken at mandibular foramen and distal to the mandibular second molar. Ramus/corpus width and height were divided into three equal parts and the proportional location of the MC was described in reference to these equal thirds. The proportional location of MC was also described in detail for the midthirds as midthird anterior/superior, midthird center, and midthird posterior/inferior (Figure 3).

MC length was measured on 3D objects derived from ideal panoramic view. Distance measurements were performed at maximum 5-mm distances, tangent to the 3D MC object along the midline by controlling axially and sagittally. The sum of these distances smaller than 5 mm comprised the actual MC length (ACL). The shortest distance between the most posterior and the most

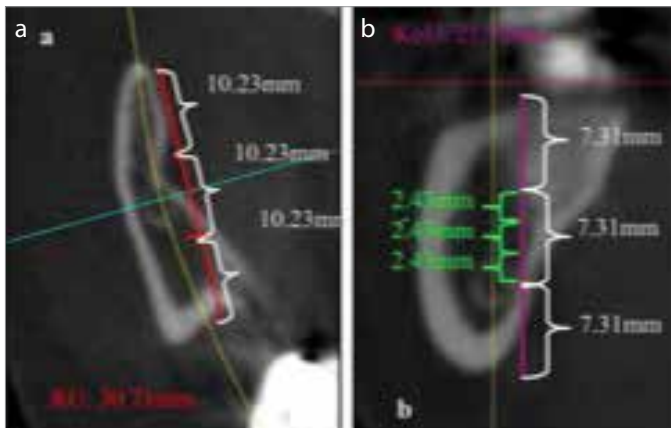


Figure 3. a, b. Proportional location of MC. on axial slice: in the midline of midthird of ramus posteroanteriorly (a); on cross-sectional slice taken distal to the mandibular second molar: in the inferior part of midthird of corpus superoinferiorly (b)

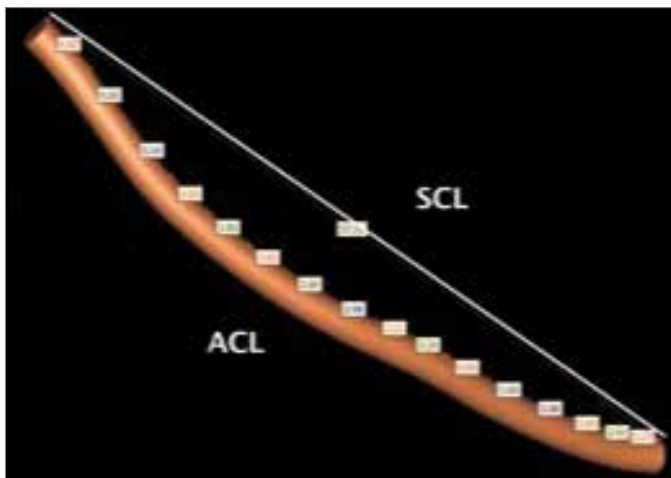


Figure 4. Measurements for actual canal length (ACL) and shortest canal length (SCL)

anterior points on the 3D object was defined as the shortest canal length (SCL) (Figure 4).

Statistical Analysis

All the steps and the measurements on 3D images of randomly chosen 13 patients were repeated 1 month after the first measurements to evaluate the reliability of the method using Intraclass Correlation Coefficient.

All data were analyzed statistically using SPSS for Windows Version 15 (SPSS Inc.; Chicago, IL, USA). Distribution of the data was analyzed using the Kolmogorov-Smirnov test. Intraclass comparison of the parameters with normal distribution were made using paired sample t-test, whereas Wilcoxon sign test was used for comparison of parameters with non-normal distribution. Results were considered as significant when $p < 0.05$.

RESULTS

Reliability of the measurements was evaluated in 95% of confidence interval, and intraclass correlation coefficient was found to be nearly 1.00 for all measurements, indicating that the measurements were reproducible with an insignificant error.

Preoperative Evaluation of Proportional Location of MC

Preoperative evaluation of proportional location of the MC showed that the mandibular foramen was located in the midthird of the ramus anteroposteriorly and superoinferiorly for most of the cases. The evaluation of the proportional location in detail showed that the mandibular foramen was located in the anterior third of the midthird. Mandibular foramen and MC were located in the inferior third of the midthird of the ramus for most of the cases.

Preoperative Location of MC in Millimeters

Preoperatively RL/CoL decreased from mandibular foramen to first molar region in both the left and right sides on cross-sectional slices. RW/CoW increased from mandibular foramen to molar region, reached its widest values on second molar region and decreased from second molar region to first molar region in both right and left sides. IL decreased and SL increased from mandibular foramen to the second molar region in both right and left sides. MC position moved inferiorly from mandibular foramen to mandibular second molar region. Both ML and LL increased from mandibular foramen to the second molar region and then decreased toward the first molar region on both right and left sides. Mean value for MCT was "0" at the inferior border of the mandibular foramen on both right and left sides, and this value slightly increased at CSM slices and decreased again at the mandibular molar region. Both on the right and left sides, LCT increased at the second molar region and slightly decreased at the CS7-6 slices. Both the CW and CL values decreased from mandibular foramen to the CS7-6 (Table 1).

Postoperative Changes in MC Location

Postoperative changes in MC location compared to the preoperative values were as follows: decreases on RL and AL and increases on RW and ML values were statistically significant on both sides in ASs. Cross-sectional first slices (CS1) showed that RW and ML were increased significantly on both sides. Cross-sectional mid slices (CSM) showed significant increases in RW, ML, and MCT on both sides. Cross-sectional slices distal to the second molar (CS7) showed significant increases in ML on both sides. No significant changes were found in CS67 slices on both sides (Table 2-6).

Postoperative Changes in MC Length

Relative postoperative changes according to the preoperative MC length were analyzed using paired t test. ACL and SCL decreased postoperatively on both right and left sides ($p < 0.01$).

DISCUSSION

The most frequent complication of BSSO is reported as IAND, which is accepted as a spontaneous outcome of this method (6, 8, 11). It may be possible to reduce IAND after BSSO through a thorough evaluation of MC location and path preoperatively (22, 23). A very detailed evaluation of IAN can be made using 3D imaging of MC (14, 21). The present study aimed to assess the location and pathway of MC both preoperatively and postoperatively, in an attempt to display the impact of BSSO on MC using 3D imaging.

Cone-beam computed tomography technique enables the clinicians to visualize the skull by using lowest radiation doses possible. However, lowering the radiation dose may compromise the visibility of structures like MC. SimPlant Pro Standalone 13.0 soft-

Table 1. Preoperative position of mandibular canal

Mean±SS(Median)				
RIGHT	CS1	CSM	CS7	CS6-7
RL/CoL	55.36±7.28	38.74±15.06	22.71±3.64	26.53±3.30
RW/CoW	11.33±1.75	14.70±2.97	17.66±2.03	15.74±2.42
IL	20.47±2.44	9.97±1.68	6.65±1.26	6.95±0.87
SL	30.60±7.18	25.32±14.60	13.09±3.14	17.08±2.89
ML	1.75±0.53	2.95±1.62	2.97±1.34	2.69±1.12
LL	3.70±1.13	4.08±1.21	5.83±1.25	5.61±1.20
MCT	0.02±0.11 (0)	0.33±0.75 (0)	0.32±0.72 (0)	0.24±0.53 (0)
LCT	0.57±0.69 (0.45)	0.61±0.64 (0.46)	2.06±1.13 (1.92)	2.00±1.15 (2.1)
CL	4.21±1.08	3.38±0.68	2.84±0.84	2.48±0.60
CW	2.40±0.62	2.03±0.42	1.84±0.49	1.58±0.27
LEFT				
RL/CoL	55.89±7.86	41.45±16.34	23.30±2.96	26.08±3.05
RW/CoW	11.47±2.12	14.55±2.31	18.46±2.22	15.83±2.16
IL	20.93±3.16	10.24±2.22	6.77±1.72	6.70±1.23
SL	30.68±7.84	27.14±15.37	13.76±2.30	16.57±2.49
ML	2.03±0.72	3.38±1.13	3.10±1.31	2.58±1.18
LL	3.90±1.22	3.99±1.01	5.89±1.29	5.67±1.40
MCT	0.00±0.00 (0)	0.41±0.62 (0)	0.35±0.61 (0)	0.24±0.48 (0)
LCT	0.67±0.86 (0)	0.49±0.72 (0.2)	2.02±1.13 (2.08)	1.89±1.20 (1.98)
CL	4.19±1.02	3.58±1.66	2.72±0.69	2.65±0.68
CW	2.40±0.59	2.01±0.48	1.88±0.39	1.71±0.40

CS1: crosssectional first slice; CSM: crosssectional mid slice; CS7: crosssectional mandibular second molar slice; CS7-6: crosssectional mandibular first and second molar slice; RL/CoL: ramus length/corpus length; RW/CoW: ramus width/corpus width; IL: inferior length; SL: superior length; ML: medial length; LL: lateral length; MCT: medial cancellous bone thickness; LCT: lateral cancellous bone thickness; CL: canal length; CW: canal width

were used in this study and the other visualization programs allow us to perform measurements on cross-sectional slices, which have been described as the most reliable slices (19). These slices are reported to be uninfluenced by the obliquity in the images (15, 17).

Evaluation of MC position, especially proportional values, gives a brief information to surgeon preoperatively. In case of high radiation risk, 3D imaging would be contraindicated. Therefore, the results obtained in this study can be used preoperatively to prevent possible manipulations of IAN during surgery. In this study, the location of MC in ASs (mandibular foramen) was found in the midthird of the ramus anteroposteriorly. Hetson et al. (22) showed it as just posterior to the midpoint of the ramus, which is similar to our results. Poonacha et al. (23) showed this location near to the posterior border of the mandible in a group aged between 3 and 13 y. The results of this study and ours seem similar considering the posterior mandibular growth of Poonacha's study group.

In the present study, location of the MC in the mandibular foramen region was found to be in the lower third of the midthird of the ramus superoinferiorly. The findings of Trebus et al. (24) and Ennes and Medeiros (25) are parallel to this finding. On the other hand, Nicholson (26) showed that MC is located in the middle of mandibular ramus superoinferiorly. The difference between our results and Nicholson's results may be due to the different reference points used in the two studies.

Thangavelu et al. (27) showed that MC was located 5 mm away from the midpoint of ramus inferiorly, which is parallel to our finding; however, it should be kept in mind that millimetric evaluations may vary between individuals. In the close proximity of the vertical osteotomy line, MC was found to be located in the midthird and less frequently in the inferior third of the corpus.

In the studies evaluating MC path, Tsuji et al. (11) and Chandak et al. (28) showed an increase in buccal cancellous bone thickness in the second molar region. This study also showed that this maximum cancellous bone thickness decreased through first molar region and the MC length and width decreased from third molar region

Table 2. Postoperative locational changes of mandibular canal on axial slices (AS)

AS(R)	Preop	Postop		AS (L)	Preop	Postop	
	Mean±SS (Median)	Mean±SS (Median)	p		Mean±SS (Median)	Mean±SS (Median)	p
RL	29.64±3.13	27.95±3.52	0.024*	RL	29.71±2.80	27.52±3.81	0.005**
RW	7.59±1.44	8.82±2.47	0.002**	RW	8.21±1.47	9.07±1.40	0.001**
PL	14.02±1.74	13.25±2.13	0.110	PL	13.76±2.13	13.51±2.14	0.447
AL	11.64±2.06	10.18±2.57	0.032*	AL	12.22±2.10	9.67±2.51	0.001**
ML	1.53±0.61	1.91±0.76	0.040*	ML	1.84±0.54	2.41±1.03	0.014*
LL	3.44±1.11	4.19±1.76	0.004**	LL	3.86±1.28	3.89±1.26	0.878
MCT	0.00±0.00 (0)	0.03±0.14 (0)	1.000	MCT	0.04±0.22 (0)	0.00±0.00 (0)	1.000
LCT	0.63±0.68 (0.5)	1.13±1.26 (0.99)	0.031*	LCT	0.71±0.89 (0)	0.58±0.82 (0)	0.286
CL	4.07±1.09	4.71±1.36	0.043*	CL	3.59±0.58	4.25±1.52	0.061
CW	2.46±0.48	2.68±0.51	0.084	CW	2.31±0.63	2.68±0.58	0.007**

Wilcoxon sign test was used for MCT and LCT, Paired Sample t test was used for other parameters (*p<0.05, **p<0.01)
 AS: axial slice; R: right; L: left; RL: ramus length; RW: ramus width; PL: posterior length; AL: anterior length; ML: medial length; LL: lateral length; MCT: medial cancellous bone thickness; LCT: lateral cancellous bone thickness; CL: canal length; CW: canal width

Table 3. Postoperative locational changes of mandibular canal on cross-sectional slices at mandibular foramen (CS1)

CS1 (R)	Preop	Postop	p	CS1 (L)	Preop	Postop	p
	Mean±SS(Median)	Mean±SS(Median)			Mean±SS(Median)	Mean±SS(Median)	
RL	55.36±7.28	53.71±6.71	0.182	RL	55.89±7.86	55.62±7.83	0.760
RW	11.33±1.75	12.52±3.12	0.034*	RW	11.47±2.12	12.47±2.49	0.009**
IL	20.47±2.44	20.54±2.62	0.859	IL	20.93±3.16	20.68±4.67	0.690
SL	30.60±7.18	27.96±7.09	0.080	SL	30.68±7.84	29.99±7.69	0.433
ML	1.75±0.53	1.88±1.08	0.560	ML	2.03±0.72	2.61±1.26	0.024*
LL	3.70±1.13	4.29±1.67	0.023*	LL	3.90±1.22	4.04±1.24	0.350
MCT	0.02±0.11 (0)	0.00±0.00 (0)	0.317	MCT	0.00±0.00 (0)	0.00±0.00 (0)	1.000
LCT	0.57±0.69 (0.45)	0.96±1.02 (0.75)	0.074	LCT	0.67±0.86 (0)	0.78±1.04 (0)	0.213
CL	4.21±1.08	5.18±1.11	0.001**	CL	4.19±1.02	4.78±1.76	0.126
CW	2.40±0.62	2.85±0.78	0.011*	CW	2.40±0.59	2.50±0.59	0.473

Wilcoxon sign test was used for MCT and LCT, Paired Sample t test was used for other parameters (*p<0.05, **p<0.01)

CS1: cross-sectional first slice; R: right; L: left; RL: ramus length; RW: ramus width; IL: inferior length; SL: superior length; ML: medial length; LL: lateral length; MCT: medial cancellous bone thickness; LCT: lateral cancellous bone thickness; CL: canal length; CW: canal width

Table 4. Postoperative locational changes of mandibular canal on cross-sectional slices at midpoint between mandibular foramen and distal point of mandibular second molar (CSM)

CSM (R)	Preop	Postop	p	CSM (L)	Preop	Postop	p
	Mean±SS(Median)	Mean±SS(Median)			Mean±SS(Median)	Mean±SS(Median)	
RL	38.74±15.06	43.38±18.60	0.093	RL	41.45±16.34	43.37±19.14	0.398
RW	14.70±2.97	15.98±2.91	0.015*	RW	14.55±2.31	15.92±2.62	0.012*
IL	9.97±1.68	9.99±2.72	0.969	IL	10.24±2.22	11.92±4.28	0.072
SL	25.32±14.60	29.12±17.77	0.147	SL	27.14±15.37	26.16±17.47	0.993
ML	2.95±1.62	4.50±2.38	0.004**	ML	3.38±1.13	5.91±2.55	0.001**
LL	4.08±1.21	4.61±1.63	0.040*	LL	3.99±1.01	4.10±1.20	0.640
MCT	0.33±0.75 (0)	1.28±1.73 (0.49)	0.017*	MCT	0.41±0.62 (0)	1.72±2.13 (0.75)	0.003**
LCT	0.61±0.64 (0.46)	0.99±1.30 (0.72)	0.211	LCT	0.49±0.72 (0.2)	0.50±0.69 (0)	0.807
CL	3.38±0.68	4.21±1.11	0.002**	CL	3.58±1.66	4.13±1.24	0.165
CW	2.03±0.42	2.23±0.60	0.133	CW	2.01±0.48	2.24±0.77	0.187

Wilcoxon sign test was used for MCT and LCT, Paired Sample t test was used for other parameters (*p<0.05, **p<0.01)

CSM: cross-sectional mid slice; R: right; L: left; RL: ramus length; RW: ramus width; IL: inferior length; SL: superior length; ML: medial length; LL: lateral length; MCT: medial cancellous bone thickness; LCT: lateral cancellous bone thickness; CL: canal length; CW: canal width

to premolar region. Nagadia et al. (29) also discussed the secure osteotomy line and their results pointed to the second molar region as others. Ozturk et al. (30) also described MC as in contact with or 2 mm away from lingual cortical bone in mandibular foramen level. This distance decreased anteriorly and MC got closer to the buccal cortical bone. Vertical evaluation showed that MC is 1 cm away from the inferior border of the mandible.

Our results were similar to the findings of the above-mentioned studies and furthermore showed the entire MC path. Moving on to the molar region from mandibular foramen region RL/CoL decreased as expected, but CoL seemed increased because of the CS7-6 slices including coronoid process. Also, RW/CoW increased from mandibular foramen to molar region and reached the maximum thickness on CS-7 slices. In the same region from mandibular foramen to molar region, MC gets closer to the inferior border superiorly and moves through cancellous bone.

From molar region to mental foramen, MC moves superiorly and buccally to reach mental foramen (Table 1).

A recent study evaluating MC position revealed that the mean distances between MC and posterior, anterior, medial, and lateral cortices at ASs were as 12.1, 11.6, 1.8, and 4.7 mm, respectively. The mean medial cancellous bone thickness was reported as 0 mm on ASs at mandibular foramen region (11, and the mean lateral cancellous bone thickness was presented as 1.96 mm (0-4.5 mm) at the same slices and region. Our results on ASs were similar to these findings as well: RL, RW, PL, AL, ML, LL, MCL, LCL, CoL, CoW as 29.7, 7.9, 13.9, 11.9, 1.6, 3.6, 0, 0.7, 3.8, and 2.4 mm, respectively. Although we found similar results, personal variations and slicing variation may affect millimetric measurements. Thus, millimetric measurements are not reliable, except when choosing the correct size of the fixation screws in order to prevent IAN injury (17).

Table 5. Postoperative locational changes of mandibular canal on cross-sectional slices at distal point of mandibular second molar (CS7)

CS7 (R)	Preop		p	CS7 (L)	Preop		p
	Mean±SS(Median)	Postop Mean±SS(Median)			Mean±SS(Median)	Postop Mean±SS(Median)	
CoL	22.71±3.64	22.28±3.42	0.330	CoL	23.30±2.96	21.97±3.08	0.016*
CoW	17.66±2.03	17.48±2.20	0.503	CoW	18.46±2.22	18.00±1.82	0.099
IL	6.65±1.26	6.33±1.31	0.273	IL	6.77±1.72	6.25±1.72	0.107
SL	13.09±3.14	13.11±3.33	0.982	SL	13.76±2.30	12.71±2.93	0.077
ML	2.97±1.34	3.71±1.75	0.040*	ML	3.10±1.31	4.21±1.98	0.015*
LL	5.83±1.25	5.44±1.49	0.079	LL	5.89±1.29	5.37±1.18	0.038*
MCT	0.32±0.72 (0)	0.49±1.02 (0)	0.445	MCT	0.35±0.61 (0)	0.59±0.91 (0)	0.314
LCT	2.06±1.13 (1.92)	1.90±1,21 (1.76)	0.266	LCT	2.02±1.13 (2.08)	1.57±1.17 (1.6)	0.117
CL	2.84±0.84	2.76±0.73	0.620	CL	2.72±0.69	3.08±0.65	0.067
CW	1.84±0.49	1.99±0.51	0.151	CW	1.88±0.39	2.06±0.55	0.218

Wilcoxon sign test was used for MCT and LCT, Paired Sample t test was used for other parameters (*p<0.05)
 CS7: crosssectional mandibular second molar slice; R: right; L: left; CoL: corpus length; CoW: corpus width; IL: inferior length; SL: superior length; ML: medial length; LL: lateral length; MCT: medial cancellous bone thickness; LCT: lateral cancellous bone thickness; CL: canal length; CW: canal width

Table 6. Postoperative locational changes of mandibular canal on cross-sectional slices at contact point between mandibular second molar and first molar (CS7-6)

CS7-6 (R)	Preop		p	CS7-6 (L)	Preop		p
	Mean±SS(Median)	Postop Mean±SS(Median)			Mean±SS(Median)	Postop Mean±SS(Median)	
CoL	26.53±3.30	26.17±3.57	0.100	CoL	26.08±3.05	25.59±3.64	0.213
CoW	15.74±2.42	15.58±2.15	0.456	CoW	15.83±2.16	15,50±2.04	0.114
IL	6.95±0.87	7.05±1.28	0.477	IL	6.70±1.23	6.66±1.69	0.889
SL	17.08±2.89	16,37±2.82	0.013*	SL	16.57±2.49	16.29±2.76	0.338
ML	2.69±1.12	2.77±1.07	0.513	ML	2.58±1.18	2.80±1.08	0.162
LL	5.61±1.20	5.19±1.30	0.002**	LL	5.67±1.40	5.22±1.47	0.065
MCT	0.4±0.53 (0)	0.20±0.48 (0)	0.249	MCT	0.24±0.48 (0)	0.14±0.24 (0)	0.499
LCT	2.00±1.15 (2.1)	1.66±1.10 (1.26)	0.017*	LCT	1.89±1.20 (1.98)	1.68±1.28 (1.6)	0.136
CL	2,48±0,60	2.75±0.74	0,087	CL	2.65±0.68	2.47±0.59	0.371
CW	1,58±0,27	1.88±0.40	0.004**	CW	1.71±0.40	1.80±0.32	0.365

Wilcoxon sign test was used for MCT and LCT, Paired Sample t test was used for other parameters (*p<0.05, **p<0.01)
 CS7-6: crosssectional mandibular first and second molar slice; R: right; L: left; CoL: corpus length; CoW: corpus width; IL: inferior length; SL: superior length; ML: medial length; LL: lateral length; MCT: medial cancellous bone thickness; LCT: lateral cancellous bone thickness; CL: canal length; CW: canal width

As a spontaneous result of BSSO setback surgery, lateral segment overlaps the medial segment. Thus, RW and ML measurements were increased, and RL and AL were decreased postoperatively. Ueki et al. (17) showed the decrease in RL and the increase in RW accordingly at the slices taken from 1 cm inferior to mandibular foramen. But they showed that AL increased and PL decreased, according to the CT images taken 1 year postoperatively, in other words, after remodeling of the MC. They stated that MC moved posteriorly and medially after remodeling. This study revealed similar results as our study about the increase in CoL and CoW, showing the stability in MC diameter, both at 10 to 22 weeks postoperatively or 1 year postoperatively (after remodeling). Therefore, we can say that the two surgeons performing our BSSO procedures did not squeeze the segments together during fixation, in order to prevent IAND.

As RW increased at ASs due to the overlapped segments, RW increased postoperatively in CS1 slices. Overlapped segments increase from mandibular foramen through molar region, thus in the same slice, the cancellous bone content of the segment increases. That is why RW, ML, and MCL increased in CSM slices.

The only postoperative alteration in CS7 was the increase in ML, indicating the minimal effect of vertical osteotomy on MC.

Evaluation of the postoperative change in the length of IAN was another aim of our study. However, CBCT imaging is a restricted method in imaging of the vessel-nerve bundle in the MC. Consequently, MC length was measured as a determinant of IAN length. These measurements showed statistically significant decreases in ACL and SCL. The original length of the inferior alveo-

lar vessel-nerve bundle is reaccommodated in the canal, which is decreased in length postoperatively.

CONCLUSION

In majority of the cases, mandibular foramen is positioned in the anterior region of the midthird of the ramus anteroposteriorly and in the inferior region of the midthird of the ramus superoinferiorly. In the close proximity of the vertical osteotomy line in the corpus, MC is located in the inferior region of the midthird of the corpus superoinferiorly.

Moving through mandibular foramen to second molar region, MC gets closer to the inferior border of the mandible superoinferiorly and gets into the cancellous bone buccolingually. Moving through second molar region to the premolar region, MC moves superiorly and buccally and reaches the mental foramen in the anterior.

Estimated MC location will be beneficial to define horizontal and vertical osteotomy lines for surgeons having restrictions for CBCT imaging.

Due to the overlapped medial and distal segments, RW and ML will increase and MC length will decrease after BSSO setback surgery. The values for postoperative changes of MC position will be used as data for a new study to correlate with IAND.

Ethics Committee Approval: Ethics committee approval was received for this study from the Non-invasive Clinical Trials Ethics Committee of the Health Sciences of Marmara University.

Informed Consent: Written informed consent was obtained from all the patients who participated in this study.

Peer-review: Externally peer-reviewed.

Author Contributions: Concept - A.A.; Design - D.İ., A.A.; Supervision - A.A.; Resources - D.İ., A.A.; Materials - D.İ., M.M., A.A.; Data Collection and/or Processing - D.İ., A.A., M.M.; Analysis and/or Interpretation - D.İ., M.M.; Literature Search - D.İ.; Writing Manuscript - D.İ.; Critical Review - A.A.

Conflict of Interest: No conflict of interest was declared by the authors.

Financial Disclosure: The authors declared that this study has received no financial support.

REFERENCES

1. Trauner R, Obwegeser H. The surgical correction of mandibular prognathism and retrognathia with consideration of genioplasty. Part I. Surgical procedures to correct mandibular prognathism and reshaping of chin. *Oral Surg Oral Med Oral Pathol* 1957; 10: 671-92. [CrossRef]
2. Wolford LM. The sagittal split ramus osteotomy as the preferred treatment for mandibular prognathism. *J Oral Maxillofac Surg* 2000; 58: 310-12. [CrossRef]
3. Epker BN. Modifications in the sagittal osteotomy of the mandible. *J Oral Surg* 1977; 35: 157-59.
4. Wolford LM, Davis WM Jr. The mandibular inferior border split: a modification in the sagittal split osteotomy. *J Oral Maxillofac Surg* 1990; 48: 92-94. [CrossRef]
5. Böckmann R, Schön P, Frotscher M, Eggler G, Lethaus B, Wolff KD. Pilot study of modification of the bilateral sagittal split osteotomy in pig mandibles. *J Craniomaxillofac Surg* 2011; 39: 169-172. [CrossRef]
6. Yoshida T, Nagamine T, Kobayashi T, Michimi N, Nakajima T, Sasakura H, et al. Impairment of the inferior alveolar nerve after sagittal split osteotomy. *J Cranio Max Fac Surg* 1989; 17: 271-78. [CrossRef]
7. Westermarck A, Bystedt H, Von Konow L. Inferior alveolar nerve function after mandibular osteotomies. *Br J Oral Maxillofac Surg* 1998; 36: 425-28. [CrossRef]
8. Muto T, Shigeo K, ts K, Kawakami J. Computed tomography morphology of the mandibular ramus in prognathism: Effect on the medial osteotomy of the sagittal split ramus osteotomy. *J Oral Maxillofac Surg* 2003; 61: 89-93. [CrossRef]
9. Kim SG, Park SS. Incidence of complications and problems related to orthognathic surgery. *J Oral Maxillofac Surg* 2007; 65: 2438-44. [CrossRef]
10. Panula K, Finne K, Oikarinen K. Neurosensory deficits after bilateral sagittal split osteotomy of the mandible-influence of sort tissue handling medial to the ascending ramus. *Int J Oral Maxillofac Surg* 2004; 33: 543-48. [CrossRef]
11. Tsuji Y, Muto T, Kawakami J, Takeda S. Computed tomographic analysis of the mandibular canal: relevance to the sagittal split ramus osteotomy. *Int J Oral Maxillofac Surg* 2005; 34: 243-246. [CrossRef]
12. Liu T, Xia B, Gu Z. Inferior alveolar canal course: a radiographic study. *Clin Oral Impl Res* 2009; 20: 1212-18. [CrossRef]
13. Tamas F. Position of mandibular canal. *Int J Oral Maxillofac Surg* 1987; 16: 65-69. [CrossRef]
14. Forni A, Sanchez-Garces MA, Gay-Escoda C. Identification of the Mental Neurovascular Bundle: A Comparative Study of Panoramic Radiography and Computer Tomography. *Implant Dent* 2012; 21: 516-21. [CrossRef]
15. Yamamoto R, Nakamura A, Ohno K, Michi K. Relationship of the mandibular canal to the lateral cortex of the mandibular ramus as a factor in the development of neurosensory disturbance after bilateral sagittal split osteotomy. *J Oral Maxillofac Surg* 2002; 60: 490-95. [CrossRef]
16. Witter G, Adeyemo WL, Beinemann J, Juergens P. Evaluation of risk injury to the inferior alveolar nerve with classical sagittal split osteotomy technique and proposed alternative surgical techniques using computer-assisted surgery. *Int J Oral Maxillofac Surg* 2012; 41: 79-86. [CrossRef]
17. Ueki K, Okabe K, Miyazaki M, Mukozawa A, Marukawa K, Nakagawa K, et al. Position of mandibular canal and ramus morphology before and after sagittal split ramus osteotomy. *J Oral Maxillofac Surg* 2010; 68: 1795-801. [CrossRef]
18. Yoshioka I, Tanaka T, Habu M, Oda M, Kodama M, Kito S, et al. Effect of bone quality and position of inferior alveolar nerve canal in continuous, long-term, neurosensory disturbance after sagittal split ramus osteotomy. *J Cranio-Maxillo-Fac Surg* 2012; 40: 178-183. [CrossRef]
19. Scarfe WC, Farman AG. What is cone-beam CT and how does it work? *Dent Clin North Am* 2008; 52: 707-30. [CrossRef]
20. Oliveira-Santos C, Capelozza ALA, Dezzoti MSG, Fischer CM, Poleti ML, Rubira-Bullen IRF. Visibility of the mandibular canal on CBCT crosssectional images. *J Appl Oral Sci* 2011; 19: 240-43. [CrossRef]
21. Aizenbud D, Ciceu C, Hazan-Moline H, Abu-El-Naaj I. Relationship between inferior alveolar nerve imaging and neurosensory impairment following bilateral sagittal split osteotomy in skeletal class III cases with mandibular prognathism. *Int J Oral Maxillofac Surg* 2012; 41: 461-68. [CrossRef]
22. Hetson G, Share J, Frommer J, Kronman JH. Statistical evaluation of the position of the position of the mandibular foramen. *Oral Surg Oral Med Oral Pathol* 1988; 65: 32-34. [CrossRef]
23. Poonacha KS, Shigli AL, Indushekar KR. Relative position of the mandibular foramen in different age groups of children: A radiographic study. *J Indian Soc Pedo Prev Dent* 2010; 28: 173-78. [CrossRef]
24. Trebus DL, Singh G, Meyer RD. Anatomical basis for inferior alveolar nerve block. *Gen Dent* 1998; 46: 632-36.
25. Ennes JP, Medeiros RM. Localization of mandibular foramen and clinical implications. *Int J Morphol* 2009; 27: 1305-11. [CrossRef]
26. Nicholson ML. A study of the position of the mandibular foramen in the adult human mandible. *Anatom Rec* 1985; 212: 110-12. [CrossRef]
27. Thangavelu K, Kannan R, Kumar NS, Retlish E, Sabitha S, Sayee Ganesh N. Significance of localization of mandibular foramen in an inferior alveolar nerve block. *J Nat Sci Biol Med* 2012; 3: 156-60. [CrossRef]
28. Chandak SO, Pandilwar PK, Bhople PR, Taori K, Chandak TO. Computed tomographic analysis of the position of the mandibular canal in unilateral temporomandibular joint ankylosis patients. *Br J Oral Maxillofac Surg* 2013; 51: 434-37. [CrossRef]
29. Nagadia R, Tay ABG, Chan LL, Chan ESY. The spatial location of the mandibular canal in Chinese: a CT study. *Int J Oral Maxillofac Surg* 2011; 40: 1401-405. [CrossRef]
30. Ozturk A, Potluri A, Vieira AR. Position and course of the mandibular canal in skulls. *Oral Surg Oral Med Oral Pathol Oral Radiol* 2012; 113: 453-58. [CrossRef]